can provide additional structural information from ^1H NMR studies. The binding constants of CrAMPPCP are similar to those of MnAMPPCP (cf. Table II). However, while with Mn^{2+} and AMPPCP two metal ions can bind simultaneously to the enzyme-bound nucleotide, thus leading to ambiguity in the analysis of the Mn^{2+} effects, the use of the exchange-inert CrAMPPCP complex overcomes this problem and may be useful in obtaining structural information with the paramagnetic reference point being only at the nucleotide metal binding site. The results obtained by using CrAMPPCP and Mn^{2+}–$Co(NH_3)_4$AMPPCP are mutually complementary, and the use of both is therefore recommended whenever possible, with enzymes which bind two metal ions at the active site.

The experimental results presented in this work support the previously proposed location for the inhibitory metal on protein kinase, i.e., as a bridge between the enzyme and the triphosphate chain of the enzyme-bound nucleotide. The finding that the distance between the γ-phosphorus of the enzyme-bound nucleotide and the serine hydroxyl oxygen of the enzyme-bound peptide is larger than 4.6 Å suggests a dissociative mechanism for the phosphoryl transfer reaction, provided that no further motion of the substrates occurs as the transition state is approached.

References

Armstrong, R. N., & Kaiser, E. T. (1978) *Biochemistry 17*, 2840.

Armstrong, R. N., Kondo, H., Granot, J., Kaiser, E. T., & Mildvan, A. S. (1979a) *Biochemistry 18*, 1230.

Armstrong, R. N., Kondo, H., & Kaiser, E. T. (1979b) *Proc. Natl. Acad. Sci. U.S.A. 76*, 722.

Bean, B. L., Koren, R., & Mildvan, A. S. (1977) *Biochemistry 16*, 3322.

Benkovic, S. J., & Schray, K. (1973) *Enzymes, 3rd Ed. 8*, 201.

Bolen, D. W., Stingelin, J., Bramson, H. N., & Kaiser, E. T. (1980) *Biochemistry 19*, 1176.

Cleland, W. W., & Mildvan, A. S. (1979) *Adv. Inorg. Biochem. 1*, 163.

Cornelius, R. D., Hart, P. A., & Cleland, W. W. (1977) *Inorg. Chem. 16*, 2799.

Demaille, J. G., Peters, J. A., & Fischer, E. H. (1977) *Biochemistry 16*, 3080.

Granot, J., Kondo, H., Armstrong, R. N., Mildvan, A. S., & Kaiser, E. T. (1979a) *Biochemistry 18*, 2339.

Granot, J., Mildvan, A. S., Brown, E. M., Kondo, H., Bramson, H. N., & Kaiser, E. T. (1979b) *FEBS Lett. 103*, 265.

Granot, J., Mildvan, A. S., Hiyama, K., Kondo, M., & Kaiser, E. T. (1980) *J. Biol. Chem. 255*, 4569.

Gupta, R. K. (1977) *J. Biol. Chem. 252*, 5183.

Gupta, R. K., Fung, C. H., & Mildvan, A. S. (1976) *J. Biol. Chem. 251*, 2421.

Kemp, B. E., Graves, D. J., Benjamini, E., & Krebs, E. G. (1977) *J. Biol. Chem. 252*, 488.

Li, T. M., Switzer, R. L., & Mildvan, A. S. (1979) *Arch. Biochem. Biophys. 193*, 1.

Mildvan, A. S. (1979) *Adv. Enzymol. Relat. Areas Mol. Biol. 49*, 103.

Mildvan, A. S., & Engle, J. L. (1972) *Methods Enzymol. 26C*, 654.

Mildvan, A. S., Sloan, D. L., Fung, C. H., Gupta, R. K., & Melamud, E. (1976) *J. Biol. Chem. 251*, 2431.

Moll, G. M., Jr., & Kaiser, E. T. (1976) *J. Biol. Chem. 251*, 3993.

Satterthwait, A., & Westheimer, F. H. (1980) *Pure Appl. Chem.* (in press).

Witt, J. J., & Roskoski, R., Jr. (1975) *Anal. Biochem. 66*, 253.

Kinetic and Chemical Mechanisms of Yeast Formate Dehydrogenase†

John S. Blanchard and W. W. Cleland*

ABSTRACT: Yeast formate dehydrogenase has an ordered kinetic mechanism with NAD adding before formate. NAD analogues are substrates, but formate is the only molecule oxidized. Anions are competitive inhibitors vs. formate and bind only to E–NAD. Linear triatomic anions are the best inhibitors, with azide (K_i = 7 nM) showing tight binding inhibition behavior and appearing to be a transition-state analogue. pH profiles of the kinetic parameters show that a group in E–NAD with a pK of 8.3 must be protonated for binding of azide and formate. Since the pK is elevated to 9.8 upon formate binding, it is probably a cationic acid involved in substrate binding. A group with pK = 6.4 and no temperature dependence must be ionized for binding of azide and formate, and another group with pK = 5.9 must be ionized for catalysis, but the roles of these groups in the mechanism are not clear. A ^{13}C isotope effect of 1.043 with either unlabeled or deuterated formate shows that formate has a very low commitment to catalysis, and all isotope effects observed are intrinsic ones on the chemical reaction. The deuterium isotope effect on $V/K_{formate}$ varies with the nature of the nucleotide, presumably as the result of changes in transition-state structure. The value of 2.8 with NAD probably results from a late transition state, while the values of 4.4 for thio-NAD, 6.9 for acetylpyridine-NAD, and 3.8 for pyridinecarboxaldehyde-NAD represent progressively earlier transition states. By contrast, the ^{13}C isotope effect drops slightly to 1.036 with acetylpyridine-NAD. These data are explained if both a higher redox potential (that is, more electrophilic C-4) for the nucleotide and an increased distance between formate and nucleotide in the transition state (indicated by a lower V_{max} and increased activation energy for the reaction) cause the transition state to become earlier.

Yeast formate dehydrogenase (formate:NAD oxidoreductase, EC 1.2.1.2) catalyzes the oxidation of formate by NAD as shown in eq 1. The enzyme will utilize a number of NAD

$$NAD^+ + HCO_2^- \rightarrow CO_2 + NADH \quad (1)$$

analogues but is apparently specific for formate. Because the reaction is essentially irreversible and involves the simple transfer of hydrogen from formate to NAD, one can simul-

† From the Department of Biochemistry, College of Agricultural and Life Sciences, University of Wisconsin–Madison, Madison, Wisconsin 53706. *Received January 14, 1980.* Supported by a grant from the National Institutes of Health (GM 18938).

0006-2960/80/0419-3543$01.00/0

taneously determine ^{13}C and ^{2}H isotope effects in order to study the mechanism of hydride transfer. In the present paper we report kinetic studies which demonstrate an ordered kinetic mechanism and isotope effect studies which show that formate has no commitment to catalysis so that the hydride transfer step is totally rate limiting for $V/K_{formate}$. The variation in isotope effects when NAD is replaced by several analogues suggests that the structure of the transition state for the reaction depends on the distance between the carbons of formate and C-4 of the nucleotide, as well as on the redox potential of the latter.

Materials and Methods

Chemicals. Yeast formate dehydrogenase, NAD (Li salt, formate free), and NADH were from Boehringer-Mannheim. Yeast and liver alcohol dehydrogenases, lactate dehydrogenase and NAD analogues were from Sigma Chemical Co. Formic acid-*1-d* (99 atom % ^{2}H) was from Merck. One millicurie of sodium [^{3}H]formate (1 mCi/mmol) from Research Products was purified by adsorption on a 1 × 5 cm column of Dowex 1-Cl and elution with a 20-mL linear gradient (0–0.4 M) of NaCl. [^{14}C]NAD (277 mCi/mmol) was from Amersham. AG-MP-1 resin was from Bio-Rad.

Sodium monothioformate was prepared by the hydrolysis of phenyl formate with sodium hydrogen sulfide in absolute ethanol (Gattow & Engler, 1971) and was purified by adsorption on a 2 × 8 cm column of Dowex 1-Cl and elution with a 200-mL linear 0–2 M NaCl gradient. Fractions containing sodium monothioformate were pooled and flashed to 5 mL. Five milliliters of 95% ethanol was added, the NaCl was removed by filtration, and ethanol was removed by rotary evaporation. The concentrations of monothioformate solutions were measured by reaction with 5,5′-dithiobis(2-nitrobenzoic acid).

Properties of the Enzyme. The molecular weight of yeast formate dehydrogenase was estimated by gel filtration on Sephadex G-100 to be 87 000 by comparison with that of glutamate dehydrogenase, yeast enolase, and myoglobin. The subunit molecular weight was 42 000 by using sodium dodecyl sulfate gel electrophoresis in 10% gels according to Weber & Osborn (1969), with bovine serum albumin, fumarase, lactate dehydrogenase, and cytochrome *c* as standards. Yeast formate dehydrogenase thus appears to be a dimer.

The activity of formate dehydrogenase was not affected by extensive dialysis against 25 mM Hepes,[1] pH 7.5, containing 10 mM EDTA and 1 mM dithiothreitol. No activation following dialysis was observed with the following metals at 10 mM concentrations (all used as the chloride salts), Fe^{2+}, Fe^{3+}, Ni^{2+}, Zn^{2+}, Co^{2+}, Mn^{2+} and Mg^{2+}, although some inhibition was observed due to the presence of chloride. No activation by monovalent cations was observed at 100 mM levels, and the spectrum of the enzyme showed no absorption in the visible region.

Initial Velocity Studies. Initial velocities were measured by monitoring the absorbance of NADH at 340 nm. Temperature was maintained between 15 and 38 °C with a circulating water bath and thermospacers. pH values were measured with a Radiometer 26 pH meter equipped with a combined microelectrode placed directly into the cuvette after data collection, and standardized at the desired temperature to ±0.01 pH unit with buffers from Beckman calibrated between 0 and 95 °C.

Solutions of formate dehydrogenase were prepared by dissolving the lyophilized powder in 0.5 mL of 25 mM Hepes, pH 7.8, 100 μM EDTA, and 100 μM dithiothreitol. This solution was applied to the top of a 1 × 12 cm column of Sephadex G-10 and eluted with the same buffer. All initial velocity studies were initiated by the addition of a small volume of cold enzyme solution to a temperature-equilibrated cuvette. The activity was stable over the measurement period at all pH values.

The following buffers were used at 100 mM concentrations at the stated pH values to allow for overlap: acetate (5.0–5.7), Mes (5.2–6.5), Pipes (6.3–7.5), Hepes (7.0–8.5), Taps (8.0–9.0), Ches (9.0–10.0), and Caps (9.5–10.4).

Determination of Substrate Concentrations. Formate-(*h,d,t*) concentrations were determined enzymatically by using 2 units of formate dehydrogenase and 5 mM NAD at pH 7.5 with 100 mM Hepes. NAD concentrations were determined by using 5 units of liver alcohol dehydrogenase and 100 mM cyclohexanol at pH 8.5 with 100 mM Taps. NADH concentrations were determined by using 5 units of lactate dehydrogenase and 5 mM pyruvate at pH 8.0 with 100 mM Hepes.

Determination of ^{3}H Isotope Effect. A 10-mL solution was made up containing 100 mM Hepes, pH 7.8, 1.4 mM [^{14}C]-NAD, and 137 μM sodium [^{3}H]formate. After temperature equilibration, a 1.0-mL aliquot was removed, and the absorbance at 340 nm measured. Formate dehydrogenase (27 units in 0.4 mL) was added to the remaining solution, and the reaction was monitored spectrophotometrically. At approximately 20, 30, and 40%, and also at 100% completion, 1-mL aliquots were removed and added to test tubes containing 0.1 mL of 2 M NaN_3 to quench the reaction. These reaction mixtures were immediately layered on 1 × 10 cm columns of AG-MP-1 (Cl form), and formate dehydrogenase, NAD, and formate were eluted with 25 mL of 0.4 M LiCl, pH 10. NADH was eluted with 25 mL of 0.65 M LiCl, pH 10, and fractions of the peak were counted in a liquid scintillation counter. The ^{3}H and ^{14}C counts in NADH were corrected for quenching, and the ratio of dpm of ^{3}H to dpm of ^{14}C was used in the calculation of $^{T}(V/K_{formate})$ by[2]

$$^{T}(V/K_{formate}) = \ln (1 - f)/\ln [1 - f(R_f/R_0)] \quad (2)$$

In eq 2, f is the fractional completion of reaction, R_f is the $^{3}H/^{14}C$ ratio at f completion, and R_0 is the $^{3}H/^{14}C$ ratio at 100% completion.

^{13}C Isotope Effects. The ^{13}C isotope effect on the formate dehydrogenase reaction was determined by the method of O'Leary (1980). Reaction mixtures contained 3 mM formate-1-(*h,d*), 3.5 mM pyruvate, 200 μM NAD, and 100 mM Hepes. The solutions were degassed with CO_2-free N_2 and titrated to pH 7.8 with saturated KOH, and the reaction was initiated by the addition of a small volume of CO_2-free buffer containing 20 units of formate dehydrogenase and 250 units of lactate dehydrogenase. The reaction was quenched at 5, 10, 15, and 100% completion by the addition of concentrated H_2SO_4, and the CO_2 was removed by distillation from a dry

[1] Abbreviations used: Hepes, *N*-2-hydroxyethylpiperazine-*N*′-2-ethanesulfonic acid; Taps, 3-[[tris(hydroxymethyl)methyl]amino]-propanesulfonic acid; Mes, 2-(*N*-morpholino)ethanesulfonic acid; Pipes, piperazine-*N*,*N*′-bis(2-ethanesulfonic acid); Ches, 2-(*N*-cyclohexylamino)ethanesulfonic acid; Caps, cyclohexylaminopropanesulfonic acid; thio-NAD, thionicotinamide adenine dinucleotide; acetylpyridine-NAD, 3-acetylpyridine adenine dinucleotide; deamino-NAD, nicotinamide hypoxanthine dinucleotide; pyridinecarboxaldehyde-NAD, 3-pyridinecarboxaldehyde adenine dinucleotide.

[2] In the nomenclature for isotope effects used here, the leading superscipt means "isotope effect on". Thus, $^{D}k_5$ is the deuterium isotope effect on k_5 (that is, k_{5H}/k_{5D}). T is used for tritium effects and 13 is used for ^{13}C effects.

Table I: Kinetic Parameters and Isotope Effects[a] in the Presence of Alternate Nucleotide Substrates at pH 7.8, 25 °C

substrate	K_m (μM)	$K_{formate}$ (mM)	rel V	^DV	rel $V/K_{formate}$	$^D(V/K_{formate})$
NAD	32	1.7	100	2.7 ± 0.1	100	2.8 ± 0.1
thio-NAD[b]	170	7.6	89	1.6 ± 0.6	20	4.4 ± 0.9
3-acetylpyridine-NAD	1160	335	4	2.1 ± 0.05	0.02	6.9 ± 0.1
deamino-NAD	540	ND[c]	1.5	ND	ND	ND
3-pyridinecarbox-aldehyde-NAD	190	30	0.2	2.4 ± 0.4	0.01	3.8 ± 0.2

[a] Formate-1-(*h*,*d*) was the variable substrate and nucleotide concentrations were saturating (>10K_m). Isotope effects on ^DV and $^D(V/K_{formate})$ were calculated from eq 10. [b] See footnote 1 for more complete names of the NAD analogues. [c] ND, not determined.

ice–2-propanol bath. The isotopic ratio of $^{13}C/^{12}C$ in CO_2 was then measured with a Nuclide Associates RMS 6-60 isotope ratio mass spectrometer with a dual-inlet system.

Data Analysis. Reciprocal initial velocities were plotted against the reciprocal of substrate concentration, and the data were fitted to appropriate rate equations by the least-squares method, assuming equal variances for the values of v, log v, or log Y, and by using a digital computer and the Fortran programs of Cleland (1979). Individual saturation curves were fitted to eq 3. Data for a sequential initial velocity pattern

$$v = \frac{VA}{K + A} \quad (3)$$

$$v = \frac{VAB}{K_{ia}K_b + K_bA + K_aB + AB} \quad (4)$$

were fitted to eq 4, while data for competitive, noncompetitive, and uncompetitive inhibition were fitted to eq 5, 6, and 7,

$$v = \frac{VA}{K(1 + I/K_{is}) + A} \quad (5)$$

$$v = \frac{VA}{K(1 + I/K_{is}) + A(1 + I/K_{ii})} \quad (6)$$

$$v = \frac{VA}{K + A(1 + I/K_{ii})} \quad (7)$$

respectively. Initial velocities obtained by varying the concentration of protio- and deuterioformate were fitted to eq 8–10, which assume isotope effects on V only, on V/K only,

$$v = VA/[K + A(1 + F_iE_V)] \quad (8)$$

$$v = VA/[K(1 + F_iE_{V/K}) + A] \quad (9)$$

$$v = VA/[K(1 + F_iE_{V/K}) + A(1 + F_iE_V)] \quad (10)$$

or on both V and V/K. When protio- and deuterioformate were varied at different levels of NAD, data were fitted to eq 11–14, which assume isotope effects on V/K_b, V and V/K_b,

$$v = \frac{VAB}{(K_{ia}K_b + K_bA)(1 + F_iE_{V/K_b}) + K_aB + AB} \quad (11)$$

$$v = \frac{VAB}{(K_{ia}K_b + K_bA)(1 + F_iE_{V/K_b}) + K_aB + AB(1 + F_iE_V)} \quad (12)$$

$$v = VAB/[(K_{ia}K_b + K_bA)(1 + F_iE_{V/K_b}) + K_aB(1 + F_iE_{V/K_a}) + AB(1 + F_iE_V)] \quad (13)$$

$$v = VAB/[[K_{ia}K_b(1 + F_iE_{K_{ia}}) + K_bA](1 + F_iE_{V/K_b}) + K_aB(1 + F_iE_{V/K_a}) + AB(1 + F_iE_V)] \quad (14)$$

V, V/K_b, and V/K_a, and V, V/K_b, V/K_a, and K_{ia}. In eq 8–14, F_i is the fraction of deuterium label in substrate, while E_V, $E_{V/K}$, E_{V/K_b}, E_{V/K_a}, and $E_{K_{ia}}$ are the isotope effect minus one for the respective parameters. The best fit was chosen on the basis of the lowest values of the standard errors of the fitted parameters and the lowest value of σ, which is the sum of the squares of the residuals divided by the degrees of freedom. Tight binding inhibition data were fitted to eq 15, where A is the concentration of active sites, E is the volume of enzyme solution added, I is the concentration of azide, and K is the inhibition constant for azide. pH profiles in which the log of the parameter plotted decreased both above pK_2 with a slope of −1 and below pK_1 with a slope of 1 were fitted to eq 16.

$$\log v = (V/2)\,[AE - I - K + [(K + AE - I)^2 + 4KI]^{1/2}] \quad (15)$$

$$\log Y = \log [c/(1 + H/K_1 + K_2/H)] \quad (16)$$

Table II: Slope Inhibition Constants vs. Formate, pH 7.8

inhibitor	K_{is} (mM)[a]
N_3^-	7.2×10^{-6}
OCN^-	83×10^{-6}
SCN^-	0.013
CN^-	0.044[b]
$HCOS^-$	0.080
NO_2^-	0.081
NO_3^-	0.27
F^-	31
Cl^-	48
Br^-	94
HCO_3^-	97

[a] Standard errors are less than 10% in all cases. [b] Inactivates at higher concentrations (Ohyama & Yamazaki, 1975).

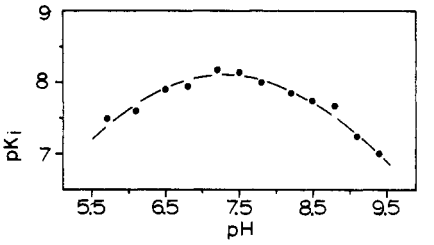

FIGURE 1: pH profile for binding of azide. Formate was the variable substrate with NAD at saturating levels. The competitive inhibition patterns were fitted to eq 5, and the resulting values of $1/K_{is}$ were fitted to eq 16 (smooth curve through the data) with pK_1 = 6.43 ± 0.06 and pK_2 = 8.27 ± 0.04.

Results

Substrate Specificity. At concentrations of at least 28 mM, formaldehyde, formamide, methanol, monothioformate, acetate, lactate, and malate were not substrates for yeast formate dehydrogenase. A number of nucleotide analogues act as substrates, and data for these are summarized in Table I. The K_m values for the nucleotides and the relative V_{max} values were determined with the same enzyme solution by varying the nucleotide concentration at a formate concentration of 300 mM.

Inhibition by Anions. A number of anions as their sodium salts were competitive inhibitors vs. formate of formate de-

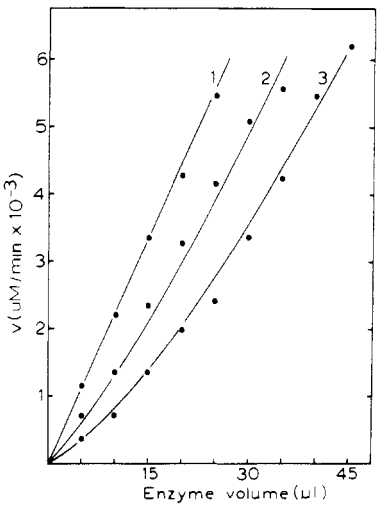

FIGURE 2: Variation in rate with enzyme concentration in the absence and presence of azide at pH 7.5. NAD, 10 mM. Formate, 1.7 mM. Azide: (1) 0, (2) 33, and (3) 66 nM. The lines are a fit to eq 15.

Table III: Product and Dead-End Inhibition at pH 8.0[a]

inhibitor	variable substrate[d]	K_{is} (mM)	K_{ii} (mM)	inhibition
NADH	NAD	0.0064 ± 0.0004		C
NADH	formate	0.0079 ± 0.0006	0.20 ± 0.16	NC
HCO_3^-	NAD	151 ± 31	1370 ± 1260	NC[b]
		124 ± 13		C
HCO_3^-	formate	97 ± 11	1385 ± 960	NC[c]
		84 ± 6		C
NO_3^-	NAD		1.25 ± 0.14	UC
NO_3^-	formate	0.334 ± 0.008		C
N_3^-	NAD		80 ± 4[e]	UC
N_3^-	formate	7.2 ± 0.5[e]		C

[a] Data fitted to eq 5-7: C, competitive; NC, noncompetitive; UC, uncompetitive. [b] Residual least square: NC, 0.00184; C, 0.00186. [c] Residual least square: NC, 0.00143; C, 0.00149. [d] Fixed substrate: formate, 10 mM, or NAD, 330 μM. [e] Units are nM.

hydrogenase at pH 7.8, and the slope inhibition constants obtained from fits of the data to eq 5 are shown in Table II. The pH variation of the pK_i for azide vs. formate at saturating NAD concentrations ($>20K_{NAD}$) is shown in Figure 1.

Tight Binding Inhibition. Since $K_{i,azide}$ is approximately equal to the enzyme concentration used in initial velocity studies, tight binding inhibition studies were carried out. Azide is a reversible inhibitor which binds as an analogue of formate, and no nonlinearity in the time course of the reaction was observed in the presence of azide. When the concentration of enzyme was varied at saturating NAD, a K_m level of formate, and 0–66 nM levels of azide, the data in Figure 2 were obtained. A fit of these data to eq 15 gave a turnover number of 248 s^{-1} at pH 7.5, extrapolated to saturating formate concentrations, and a $K_{i,azide}$ of 28 nM.

Initial Velocity Studies at pH 8.0. When formate was varied at several fixed levels of NAD, an intersecting initial velocity pattern was obtained, indicating a sequential kinetic mechanism. From a fit of the data to eq 4, K_{NAD} = 32 ± 5 μM, $K_{i,NAD}$ = 223 ± 31 μM, and $K_{formate}$ = 1.76 ± 0.26 mM. Product inhibition patterns for NADH and bicarbonate, and dead-end inhibition patterns for azide and nitrate vs. formate and NAD are summarized in Table III, along with the inhibition constants from fits to eq 5–7.

pH Profiles of the Kinetic Parameters. When NAD was varied at saturating levels of formate (over $20K_{formate}$) and the data were fitted to eq 3, the V/K_{NAD} profile decreased at both high pH and low pH (Figure 3). When formate was varied at saturating levels of NAD (over $30K_m$) and the data were fitted to eq 3, the profiles for $V/K_{formate}$ and V seen in Figure 3 were obtained.

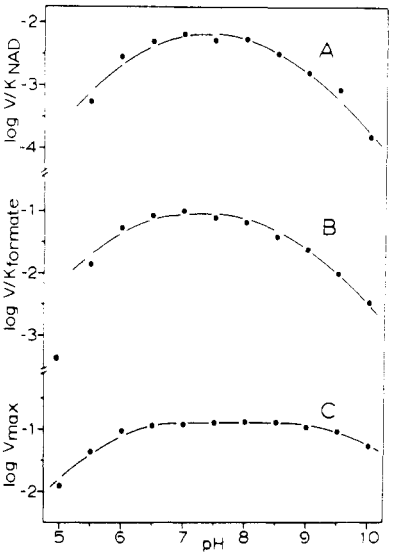

FIGURE 3: pH profiles of the kinetic parameters. The data at each pH were fitted to eq 3, and the resulting values were fitted to eq 16 (smooth curve through the data). (A) NAD was the variable substrate and formate was kept at saturating levels: pK_1 = 6.42 ± 0.07 and pK_2 = 8.41 ± 0.06. (B and C) Formate was the variable substrate and NAD was kept at saturating levels. For the V/K profile, pK_1 = 6.10 ± 0.06 and pK_2 = 8.52 ± 0.05, while for the V profile, pK_1 = 5.89 ± 0.02 and pK_2 = 9.82 ± 0.04.

Temperature Dependence of pK Values in the $V/K_{formate}$ and V Profiles. The enthalpies of ionization of the groups with low pK and high pK were calculated from an Arrhenius plot of pK vs. $1/T$ for pK values from pH profiles for $V/K_{formate}$ determined at 19, 25, 31, and 38 °C and fitted to eq 16. The pK_1 values of 5.86 ± 0.02, 5.98 ± 0.05, 6.06 ± 0.05, and 5.93 ± 0.10 at the four temperatures gave a ΔH_{ion} of −2.5 ± 1.8 kcal/mol, while the values of 9.02 ± 0.02, 8.84 ± 0.05, 8.39 ± 0.05, and 8.09 ± 0.09 for pK_2 gave a ΔH_{ion} of 20 ± 2 kcal/mol. For the V profiles, pK_1 values of 5.83 ± 0.03, 5.60 ± 0.03, 5.73 ± 0.03, and 5.58 ± 0.04 at the four temperatures gave a ΔH_{ion} of 4.6 ± 2.0 kcal/mol, while values for pK_2 of 10.53 ± 0.07, 10.6 ± 0.2, 9.48 ± 0.05, and 9.25 ± 0.06 gave a ΔH_{ion} of 29 ± 5 kcal/mol.

Temperature Dependence of V and $V/K_{formate}$. These parameters were determined at 15, 20, 25, 30, and 35 °C by varying formate at saturating levels of NAD or acetylpyridine-NAD. The activation energies calculated from Arrhenius plots were 8.6 ± 0.5 and 10.9 ± 0.3 kcal/mol for $V/K_{formate}$ with NAD and acetylpyridine-NAD, respectively. The value for V was 15.1 ± 0.5 kcal/mol with NAD, but V values with acetylpyridine-NAD could not be determined precisely enough to get a meaningful value.

Deuterium Isotope Effects. When formate-*1*-(*h,d*) was varied at several levels of NAD at pH 7.8, significant isotope effects were observed only on V (2.33 ± 0.22) and $V/K_{formate}$ (3.42 ± 0.49). This experiment was repeated at pH 9.8, and again significant isotope effects were only observed on V and $V/K_{formate}$. When formate-*1*-(*h,d*) was varied at saturating concentrations of NAD, significant isotope effects were obtained at all pH values between 5.5 and 10.4 (Figure 4). $^D(V/K_{formate})$ is pH independent with an average value of 2.8, while ^DV increased from 2 at pH 5.5 to 2.8 at pH 7 and then decreased rapidly above pH 9. Yeast formate dehydrogenase will utilize a number of alternate nucleotide substrates, and

Table IV: ^{13}C Isotope Effects at pH 7.8, 25 °C

nucleotide	formate ([?]CO_2^-)	% reaction[a]	isotope ratios[b] ($\times 10^5$) low conversion	isotope ratios[b] ($\times 10^5$) 100% conversion	$^{13}(V/K_{formate})$[c]
NAD	H	5.47	1285.77	1339.54	1.0431
		8.56	1287.83	1339.66	1.0421
		14.89	1290.00	1339.65	1.0417
NAD	D	9.70	1291.51	1347.37	1.0455
		15.74	1297.59	1347.25	1.0417
acetylpyridine-NAD	H	9.2	1223.83	1265.11	1.0353
		10.0	1222.43	1265.11	1.0368

[a] Determined by recovery of CO_2 from the acidified reaction mixtures. [b] Decade settings for m/e 45/44 corrected to tank standard = 1260. [c] Isotope effects are calculated from eq 2.

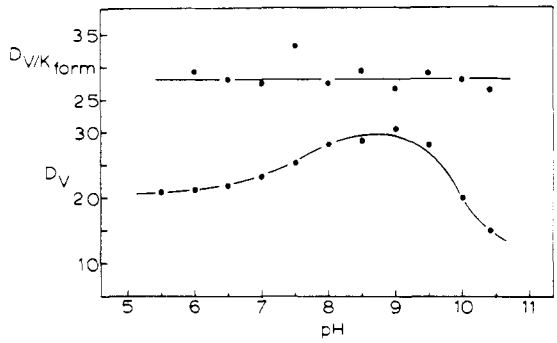

FIGURE 4: pH variation of the primary isotope effects. Formate-*1*-(*h*,*d*) was the variable substrate and NAD was kept at saturating levels. The data were fitted to eq 8–10, and the best fit was chosen on the basis of the lowest residual least square and the lowest standard errors of the fitted parameters.

the isotope effects observed on V and $V/K_{formate}$ for a number of these are shown in Table I.

^3H Isotope Effects. The ^3H isotope effect, determined by measuring the $^3H/^{14}C$ ratio in NADH as a function of fractional completion with formate-1-*t* and [^{14}C]NAD as substrates, was 4.9 ± 0.1.

^{13}C Isotope Effects. When the ^{13}C isotope effect was measured with protio- and deuterioformate, the data in Table IV were obtained. The average $^{13}(V/K_{formate\text{-}h})$ was 1.0423 and $^{13}(V/K_{formate\text{-}d})$ was 1.0436 with NAD as the coenzyme, but the isotope effect was 1.0360 with acetylpyridine-NAD and unlabeled formate.

Discussion

Substrate Specificity. Yeast formate dehydrogenase is specific for formate, and no other oxidizable substrates have been found for the yeast enzymes from either *Candida boidinii* (Schütte et al., 1976) or *Kloeckera* sp. (Kato et al., 1974). The replacement of one of the oxygen atoms with sulfur results in a complete loss of activity, although monothioformate can bind to the enzyme–NAD complex with a K_i of 80 μM. All uncharged formate analogues, including formamide, formaldehyde, and methanol, neither undergo catalysis nor bind to the enzyme–nucleotide complex.

The yeast enzyme will, however, utilize a number of nucleotides in place of NAD, although all tested have higher Michaelis constants and lower maximum velocities. No activity was detected at concentrations in excess of 1 mM with NADP, dichlorophenolindophenol, methylviologen, or methylene blue.

Inhibition by Anions. All of the anions tested were linear competitive inhibitors vs. formate, but it is apparent from Table II that there is a wide variation in the affinity of the various anions for the E–NAD complex. The most effective inhibitors are linear triatomic anions, while the trigonal tetratomic anions are considerably poorer inhibitors. Azide is the most effective inhibitor tested; the slope inhibition constant of azide is 500000 times lower than the Michaelis constant of formate. Azide is an inhibitor of all formate dehydrogenases studied to date (Thauer et al., 1977), an observation which has prompted the suggestions that all formate dehydrogenases are metalloenzymes and that the inhibition by azide is due to liganding to metals. An order of affinity of monovalent anions similar to that observed in this study has been reported for the reduced ferredoxin: CO_2 reductase of *Clostridium pasteurianum* (Thauer et al., 1975), which is known to contain molybdenum and iron–sulfur centers (Scherer & Thauer, 1978). Further, this same order is observed for the stability of complexes of these anions with transition metals such as Fe, Zn, and Mo (Ahrland et al., 1958). However, the inhibition constants for azide measured with purified formate dehydrogenases known to contain Mo and Fe vary from 4 μM (Thauer et al., 1975) to millimolar levels (Enoch & Lester, 1975), whereas azide binds to the yeast enzyme with a K_i of 7 nM. Further, while the *C. pasterianum* enzyme is rapidly inactivated in the presence of oxygen, the yeast enzyme is not, and no precautions have been taken in these studies to exclude atmospheric oxygen. No loss of activity is observed upon 48-h dialysis against 10 mM EDTA, and no increased activity is observed upon the addition of metals to the dialyzed enzyme. Although these criteria cannot rule out tightly bound metal, there is no positive evidence that the yeast enzyme contains metal. We feel that the tight binding of azide to the E–NAD complex is probably due to some other factor than its ability to form strong ligand bonds to metals and that azide is acting as a transition-state analogue. We will discuss the possible reasons for this below.

The curved plots obtained by titrating enzyme activity with azide, Figure 2, have been observed previously for dihydrofolate reductase in the presence of the tight binding inhibitor, methotrexate (Williams & Morrison, 1979). The turnover number we calculate of 248 s^{-1} can be compared with values of 800, 310, and 500 s^{-1} for the oxidation of formate by enzymes from *C. pasteurianum* (Scherer & Thauer, 1978), *Escherichia coli* (Enoch & Lester, 1975), and *Vibrio succinogenes* (Kröger & Innerhofer, 1976), respectively.

Kinetic Mechanism. The intersecting initial velocity pattern when formate and NAD are varied indicates that the kinetic mechanism of yeast formate dehydrogenase is sequential. The product and dead-end inhibition patterns in Table III are consistent with a steady-state ordered kinetic mechanism in which NAD binds first, since the uncompetitive inhibition of nitrate or azide vs. NAD indicates that these analogues bind only to the E–NAD complex. In an ordered mechanism V/K_a is the bimolecular rate constant for binding of A, and no isotope effect is predicted for this parameter (Cleland, 1977). Significant isotope effects were observed at pH 7.8 and 9.8 only on V and $V/K_{formate}$, as expected in an ordered mechanism.

pH Profiles. Since V/K_{NAD} is the bimolecular rate constant for addition of NAD to free enzyme, its pH profile will show the pK values of free enzyme (the pK values of NAD are below the experimentally accessible region). The binding of NAD is prevented by protonation of a group with pK 6.42 and by deprotonation of a group with pK 8.41. It is not clear what groups these are. While their pK values are similar to those seen in the other pH profiles, if the mechanism is ordered, formate or azide should select the properly protonated form of E–NAD, and thus the pK values of free enzyme should not appear in the pH profile for $pK_{i,azide}$ or $V/K_{formate}$.

In the pH profile of pK_i for an inhibitor, decreases are seen whenever a group on either the inhibitor or the enzyme must be in the correct protonation state for binding, and because the K_i value is an equilibrium dissociation constant, correct pK values are seen in the profile. The pK values in the pK_i profile for azide represent ionizable groups in the enzyme–NAD complex, since azide does not bind to free enzyme, and neither pK corresponds to that of azide (4.72). Thus, the binding of azide is prevented when a group with a pK of 6.4 in the E–NAD complex is protonated or when a group with a pK of 8.3 in the E–NAD complex is deprotonated.

If formate binds only to the E–NAD complex, the pK values in the $V/K_{formate}$ profile should be the same as those in the pK_i profile for azide, and this is the case. The pK values do not appear to be displaced outward on the profile (Cleland, 1977) in the manner expected if formate were sticky (that is, dissociates more slowly than it undergoes conversion to CO_2). However, it appears that there may be two or more pK values at low pH, since the curve appears to drop with an eventual slope of at least 2. One of these groups is presumably that seen in the pK_i profile for azide, while another may be that seen in the V profile (see below).

The pK values in the V profile are those of groups on the enzyme with both substrates bound. The high pK is displaced outward by 1.35 pH units, while the low pK is shifted outward by 0.5 pH unit from those in the pK_i profile for azide. This unequal displacement may result from the two pK values at low pH postulated above. If the pK responsible for binding formate or azide were also to be displaced by 1.35 pH units, it would be seen at pH 5, and indeed the point at pH 5 in the V profile lies below the fitted curve. The pK of 5.9 would thus not be displaced from its value in the $V/K_{formate}$ profile and must be related to catalysis rather than to binding.

Identification of Groups Corresponding to pK Values in pH Profiles. The pH profiles discussed above show that a group with a pK of 6.4 must be deprotonated, that a group with a pK of 8.4 must be protonated for binding of azide and formate, and that a group with a pK of 5.9 must be deprotonated for catalysis. The temperature dependence of the pK of 6.4 in the $V/K_{formate}$ profile suggests that it corresponds to a carboxylic acid residue, while the enthalpic behavior of the high pK in both $V/K_{formate}$ profiles and its displacement by 1.35 pH units upon formate binding suggests a cationic acid residue such as lysine. The abnormally high ΔH_{ion} is possibly due to a conformation change which accompanies the deprotonation of this group. The temperature dependence of the group with a pK of 5.9 in the V profile is unfortunately too uncertain for identification.

The role of the carboxylic acid with a pK of 6.4 in binding and the group with a pK of 5.9 in catalysis is not clear, although presumably neither group acts as a base, since no protons are removed from the substrate prior to or during dehydrogenation. The group with a pK of 8.4 may hydrogen bond to one or both of the oxygens of formate, since only anions show affinity for the active site, and since the binding of formate elevates the pK of this group by 1.35 pH units.

Interpretation of Isotope Effects. In an ordered mechanism where A, B, P, and Q are NAD, formate, CO_2, and NADH:

$$E \underset{k_2}{\overset{k_1A}{\rightleftharpoons}} EA \underset{k_4}{\overset{k_3}{\rightleftharpoons}} EA' \underset{k_6}{\overset{k_5B}{\rightleftharpoons}} EA'B \underset{k_8}{\overset{k_7}{\rightleftharpoons}} EPQ' \underset{k_{10}P}{\overset{k_9}{\rightleftharpoons}} EQ' \xrightarrow{k_{11}} EQ \xrightarrow{k_{13}} E \quad (17)$$

k_7 and k_8 are the isotope sensitive steps and all other steps are isotope independent; the deuterium isotope effects are given by

$$^{D}(V/K_b) = \frac{^{D}k_7 + c_f + c_r{}^{D}K_{eq}}{1 + c_f + c_r} \quad (18)$$

$$^{D}V = \frac{^{D}k_7 + c_{Vf} + c_r{}^{D}K_{eq}}{1 + c_{VT} + c_r} \quad (19)$$

where

$$c_f = k_7/k_6 \quad (20)$$

$$c_r = k_8/k_9 \quad (21)$$

$$c_{VT} = k_7(1/k_3 + 1/k_9 + 1/k_{11} + 1/k_{13}) \quad (22)$$

$$^{D}K_{eq} = k_{7H}k_{8D}/(k_{7D}k_{8H}) \quad (23)$$

Equations 18, 20, 21, and 23 also apply for tritium and ^{13}C effects (with T or 13 replacing D), but since these are used as trace labels, one can not determine ^{T}V or ^{13}V.

The measurement of ^{13}C isotope effects with an isotope ratio mass spectrometer can be accomplished with a high degree of precision, and the product of the formate dehydrogenase reaction, CO_2, is ideally suited for mass spectrometric analysis. Thus, if formate had a finite commitment to catalysis (that is, c_f or c_r as given by eq 20 and 21 were finite), the ^{13}C isotope effect obtained with deuterioformate should be larger than that with protioformate, since k_{7D} and k_{8D} rather than k_{7H} and k_{8H} will occur in eq 20 and 21, and c_f and c_r will be smaller by $^{D}k_7$ and $^{D}k_8$. No significant difference was observed between $^{13}(V/K_{formate\text{-}h})$ and $^{13}(V/K_{formate\text{-}d})$, and thus c_f and c_r are zero at pH 7.8, and the intrinsic ^{13}C isotope effect on the oxidation of formate to CO_2 is 1.043 [for comparison, the decarboxylation of formate catalyzed by formate dehydrogenase isolated from *Clostridium* sp. showed a ^{13}C isotope effect of 1.026 (Hoering, 1961)]. These results require that $^{D}k_7$ equal the observed $^{D}(V/K_{formate})$ value of 2.8. The observation that $^{D}(V/K_{formate})$ is pH independent also suggests that k_7/k_6 is very small and that formate is not sticky. Intrinsic tritium isotope effects are expected to be the 1.442 power of the deuterium ones (Swain et al., 1958) and $2.8^{1.442} = 4.4$, which is in fair agreement with the observed $^{T}(V/K_{formate})$ of 4.9.

When NAD was replaced with several analogues, the observed deuterium isotope effects were all larger than those with NAD (Table I). It seems unlikely that the commitment to catalysis for formate is larger with these substrates than with NAD, as the apparent $K_{formate}$ is higher than with NAD and the V values are lower. Thus, the $^{D}(V/K_{formate})$ values are presumably intrinsic deuterium isotope effects on k_7 in mechanism 17. We can interpret these results in terms of the transition-state structure shown in Figure 5.

The hydride transfer is induced by carbonium ion character at C-4 of the nucleotide, and the secondary isotope effect studies of Cook (1980) have strongly suggested that for alcohol dehydrogenases, at least, the positive charge is made to move

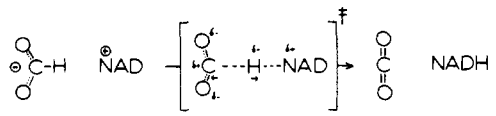

FIGURE 5: Proposed transition-state structure for the formate dehydrogenase catalyzed oxidation of formate.

from N-1 to C-4 of the nicotinamide ring by bending the N-1 to ribose bond so that N-1 becomes nearly tetrahedral, as opposed to its normal trigonal geometry.[3] During the hydride transfer, both the hydrogen and carbon of formate move in opposite directions (we presume that the oxygens of formate are held by the enzyme and are not free to move appreciably), unlike the usual situation in dehydrogenases where the carbon of the substrate probably undergoes much less motion. The intrinsic deuterium isotope effect of 2.8, which is relatively low compared with reported values of 5–8 for malic enzyme (Schimerlik et al., 1977) and 5.5–6 for alcohol dehydrogenases (P. F. Cook, unpublished experiments), does not result from this, however, since values as high as 6.9 are seen with NAD analogues. Rather, we believe the value of 2.8 reflects a late transition state (that is, one in which the geometry is close to that of the products, NADH and CO_2, rather than being midway between that of substrates and that of products).[4] This conclusion is supported by the relatively large ^{13}C effect of 1.043 and by the behavior of azide as a transition-state analogue. Azide, with its full positive charge at N_2, full negative charges at N_1 and N_3, and linear structure, fulfills all of the requirements for the predicted transition state. Cyanate, with a full negative charge on oxygen and linear structure, but only δ^+ and δ^- charges on carbon and nitrogen due to electronegativity differences, binds 10 times more poorly than azide. Linear and symmetrically charged anions are thus the best analogues of the transition state.

While a definitive explanation for the variation in intrinsic $^D(V/K_{formate})$ values with the nature of the nucleotide cannot be given at this time, the higher deuterium isotope effects with NAD analogues can be explained by a combination of effects which produce an earlier (that is, more reactant-like) transition state. The work of Stewart & Toone (1978) on the oxidation of formate to CO_2 by a series of carbonium ions in 71% aqueous trifluoroacetic acid shows that the primary deuterium isotope effect varies from 1.8 to 3.2 and shows a maximum when plotted vs. pK_{R^+} for the carbonium ion. We suggest that the increasing values of 4.4 and 6.9 for thio-NAD and acetylpyridine-NAD represent progressively earlier transition states, with the latter value probably corresponding to the maximum value, and that the value of 3.8 for pyridinecarboxaldehyde-NAD represents a still earlier transition state which more nearly resembles the substrates than the products.[4]

We believe two effects are responsible for the earlier transition states with NAD analogues. First, the redox potentials of thio-NAD, pyridinecarboxaldehyde-NAD, and acetylpyridine-NAD are −0.285, −0.262, and −0.258 V at pH 7, while that of NAD is −0.320 V (Kaplan, 1960). The reaction is thus more thermodynamically favorable with these analogues, and this will produce an earlier transition state because of the more electrophilic nature of the nucleotide. This is certainly the major effect with thio-NAD, which has nearly the same V as NAD.

The second effect is the lengthening reaction path along which the hydrogen must move during the reactions which show lower V values as a result of higher energies of activation. As the distance between formate and the C-4 of the nucleotide gets larger, the transition state necessarily gets earlier since the C–H bond of formate can only be stretched so far before it breaks. This effect is not important for thio-NAD, which has nearly the same V as NAD, but is clearly the major effect with acetylpyridine-NAD, and even more so with pyridinecarboxaldehyde-NAD. In these cases the enzyme apparently does not fully undergo the conformation change which brings the reactants together and reduces the activation energy. In support of this explanation, the activation energy for $V/K_{formate}$ is 2.3 kcal/mol higher with acetylpyridine-NAD than with NAD. $V/K_{formate}$ in the present case where the commitment to catalysis of formate is very low is simply the ratio of V and the dissociation constant of formate, and while the latter is temperature dependent and clearly higher with the lower nucleotides than with NAD, the temperature dependence of $K_{formate}$ will probably not differ with the nucleotide, and the V values with the two nucleotides should also have activation energies which differ by 2.3 kcal/mol.

Note that the ^{13}C isotope effect does not increase in going from NAD to acetylpyridine-NAD, as the deuterium effect does, but decreases slightly from 4.3 to 3.6%. While an atom which is transferred during a reaction, and thus forms a new bond as the old one is broken, shows small isotope effects for very early or very late transition states and a maximum value for a transition state that is intermediate in structure (Sims et al., 1972), the isotope effects for an atom which is part of the leaving group, and thus does not form a new bond to compensate for the one being broken, are small for early transition states and increase without a maximum, with the highest value seen for a very late transition state (Sims et al., 1972). When such an atom strengthens its remaining bonds to compensate partially for the one being broken, as the carbon of formate does here, the curve of isotope effect vs. bond order of the newly forming nucleotide–hydrogen bond might be expected to be concave downward without a maximum, but rising steeply at very early transition states to a plateau with little slope. The two observed ^{13}C isotope effects are consistent with such a picture, but only further experimental and theoretical work can tell whether it is entirely correct or not.

pH Variation of ^DV. If $^D(V/K_{formate}) = {}^Dk_7$ and c_f and c_r in eq 20 and 21 are very small, ^DV will be reduced from $^Dk_7$ only as a result of c_{VT}, and thus the observed changes in Figure 4 show that c_{VT} is very small between pH 8 and pH 9 but increases precipitously above pH 10 to a value ~3 and increases below pH 8 to a level of ~0.8. It is thus clear that at least one of the forward unimolecular rate constants k_3, k_9, k_{11}, or k_{13} decreases at low and high pH relative to k_9 in such a fashion that c_{VT} increases from a value less than 0.2 to the high values quoted above, but we cannot at this time tell which one or ones are responsible.

Acknowledgments

We thank Dr. Marion H. O'Leary and Dr. James E. Rife for their help with determination of the ^{13}C isotope effects and

[3] Recent experiments by Dr. Paul Cook in this laboratory have yielded similar results with formate dehydrogenase. Thus, NAD-*4-d* shows an isotope effect of 1.22 on $V/K_{formate}$ (1.37 from the NADH side because of the equilibrium isotope effect), which strongly suggests a carbonium ion intermediate at C-4 of the nicotinamide ring.

[4] It may be that this transition state appears later than it really is. The calculations of Sims et al. (1972) show that when the group transferred during the reaction (carbon in their calculations, but the same should hold true for hydrogen) forms a stronger bond with the entering group than with the leaving group, the maximum primary isotope effect occurs at an early transition state where the bond order to the incoming group is smaller than 0.5. Since hydrogen is more stiffly bonded in NADH than in formate [fractionation factors of 0.98 and 0.80 relative to water (Cleland, 1980)], the maximum value should occur for an early transition state rather than for a symmetrical one.

Dr. Leslie B. Sims for helpful discussions.

References

Ahrland, S., Chatt, J., & Davies, N. R. (1958) *Q. Rev. Chem. Soc. 12*, 265.
Cleland, W. W. (1977) *Adv. Enzymol. Relat. Areas Mol. Biol. 45*, 273.
Cleland, W. W. (1979) *Methods Enzymol. 63*, 103.
Cleland, W. W. (1980) *Methods Enzymol. 64*, 104.
Cook, P. F. (1980) *Fed. Proc., Fed. Am. Soc. Exp. Biol. 39*, 1641.
Enoch, H. G., & Lester, R. (1975) *J. Biol. Chem. 250*, 6693.
Gattow, G., & Engler, R. (1971) *Angew. Chem., Int. Ed. Engl. 10*, 415.
Hoering, T. C. (1961) *Pap. Geophys. Lab., Carnegie Inst. Washington 1363*, 200.
Kaplan, N. O. (1960) *Enzymes, 2nd Ed. 3*, 105.
Kato, N., Tani, Y., & Ogata, K. (1974) *Agric. Biol. Chem. 38*, 675.
Kröger, A., & Innerhofer, A. (1976) *Eur. J. Biochem. 69*, 487.
Ohyama, T., & Yamazaki, I. (1975) *J. Biochem. (Tokyo) 77*, 845.
O'Leary, M. H. (1980) *Methods Enzymol. 64*, 83.
Scherer, P. A., & Thauer, R. K. (1978) *Eur. J. Biochem. 85*, 125.
Schimerlik, M. I., Grimshaw, C. E., & Cleland, W. W. (1977) *Biochemistry 16*, 571.
Schütte, H., Flossdorf, J., Sahm, H., & Kula, M.-P. (1976) *Eur. J. Biochem. 62*, 151.
Sims, L. B., Fry, A., Netherton, L. T., Wilson, J. C., Reppond, K. D., & Crook, S. W. (1972) *J. Am. Chem. Soc. 94*, 1364.
Stewart, R., & Toone, T. W. (1978) *J. Chem. Soc., Perkin Trans. 2*, 1243.
Swain, C. G., Stivers, E. C., Renwer, J. F., Jr., & Schaad, K. J. (1958) *J. Am. Chem. Soc. 80*, 5885.
Thauer, R. K., Fuchs, G., & Kaufer, B. (1975) *Hoppe-Seyler's Z. Physiol. Chem. 356*, 653.
Thauer, R. K., Fuchs, G., & Jungermann, K. (1977) in *Iron-Sulfur Proteins* (Lovenberg, W., Ed.) Vol. III, p 121, Academic Press, New York.
Weber, K., & Osborn, M. (1969) *J. Biol. Chem. 244*, 4406.
Williams, J., & Morrison, J. (1979) *Methods Enzymol. 63*, 437.

Thermodynamics and Kinetics of Bovine Neurophysins Binding to Small Peptide Analogues of Oxytocin and Vasopressin†

A. Frances Pearlmutter* and Ellen J. Dalton

ABSTRACT: Thermodynamic binding constants for the interactions of mononitrated neurophysins with oxytocin, vasopressin, and peptide analogues of the hormones were determined by using a spectrophotometric titration technique. The data were fit to a binding model which included all known interactions in these systems. From an examination of the free energies for the binding reaction, we concluded that residues 1–3 contribute 84% of the binding energy for formation of the neurophysin dimer mono complex and 79% for the formation of the bis complex. Rate constants for complex formation and dissociation with native bovine neurophysin were determined by using temperature-jump relaxation. The association rate constants for neurophysin dimer binding to oxytocin, vasopressin, and the peptide analogues were all in the range of 1.3 $\times 10^6$ M^{-1} s^{-1} for mono complexation and 1.5 $\times 10^6$ M^{-1} s^{-1} for bis complexation. Thus, formation rate constants are identical for both mono and bis complexation, and no significant differences exist between formation constants for hormones and peptides. On the other hand, a clear distinction in dissociation rate constants is apparent when one compares the hormones (k_r = 4 to 16 s^{-1}) with the peptide analogues (k_r = 54 to 182 s^{-1}). There is roughly a tenfold increase in overall dissociation rate constant when one compares the peptides to the hormones. From these data, we conclude that the rate-determining step in the association reaction involves the first two or three residues on the hormone. After the initial binding takes place, only with intact hormone, i.e., oxytocin or vasopressin, can additional bonding interactions in the complex take place. These additional interactions are reflected in the slower off-rate of the hormone complexes relative to the peptide complexes.

The neurohypophyseal hormones, oxytocin and vasopressin, are stored in granules in the posterior pituitary in a covalent association with a binding protein, neurophysin. In the cow, two neurophysins of closely related structure are found, bovine neurophysin I, which is associated with vasopressin, and bovine neurophysin II, associated with oxytocin. In vitro, each neurophysin is capable of association with either hormone with similar binding affinity. Indirect evidence (Brownstein & Gainer, 1977; Gainer & Brownstein, 1977; Lauber et al., 1979) indicates that the bovine neurophysins and the hormones are synthesized as part of a larger precursor, which is cleaved to form the neurophysin and its associated hormone, which are then stored in granules.

The neurophysin–hormone system is an ideal vehicle for studying protein–hormone interactions; neurophysins are readily purified and oxytocin, vasopressin, and peptide analogues of the hormones are available. The amino acid sequences of the bovine neurophysins are known (Walter et al., 1971; North et al., 1975; amended by Wuu & Crumm, 1976).

† From the Department of Biochemistry, Medical College of Ohio, Toledo, Ohio 43699. *Received January 2, 1980.* This research was supported by a grant from the National Institutes of Health (AM18383) and Biomedical Research Support Grant S07 RR 05700 08.

0006-2960/80/0419-3550$01.00/0